Northwest Hydraulic Consultants Inc.
301 W. Holly Street, Suite U3
Bellingham, WA 98225
Tel: 206.241.6000

NHC Reference No. 2009321
May 13, 2025

To: Kittitas County and Inter-Fluve, Inc.

Re: Lower Kittitas Reach Floodplain Reconnection Project
Existing Conditions and Geomorphic Characterization Draft Report, Rev. 2

1 INTRODUCTION

This memo summarizes existing geomorphic conditions and characterizations on the Yakima River at and near the Lower Kittitas Restoration Project. The memo includes field observations of the channel and floodplain, review of background information, and characterization of existing geomorphic conditions and processes. The purpose of this memo is to assist the design team in defining hydraulic modeling needs and refining concept designs based on reach morphodynamics and expected channel response. This work is being conducted by NHC for Kittitas County and Inter-under subcontract to Inter-Fluve.

The project area extends along about 3 miles of the Yakima River, just above the point where it exits the alluvial Kittitas Valley and enters the Yakima River Canyon, which is cut through bedrock of Manashtash Ridge (Figure 1.1). It encompasses about 475 acres of the left bank floodplain which presently includes areas of gravel pits, agricultural land use, riparian cottonwood forest, and a decommissioned RV park. The geomorphic reach assessment extended from the Umptanum Road crossing to the Ringer Road Boat Ramp.

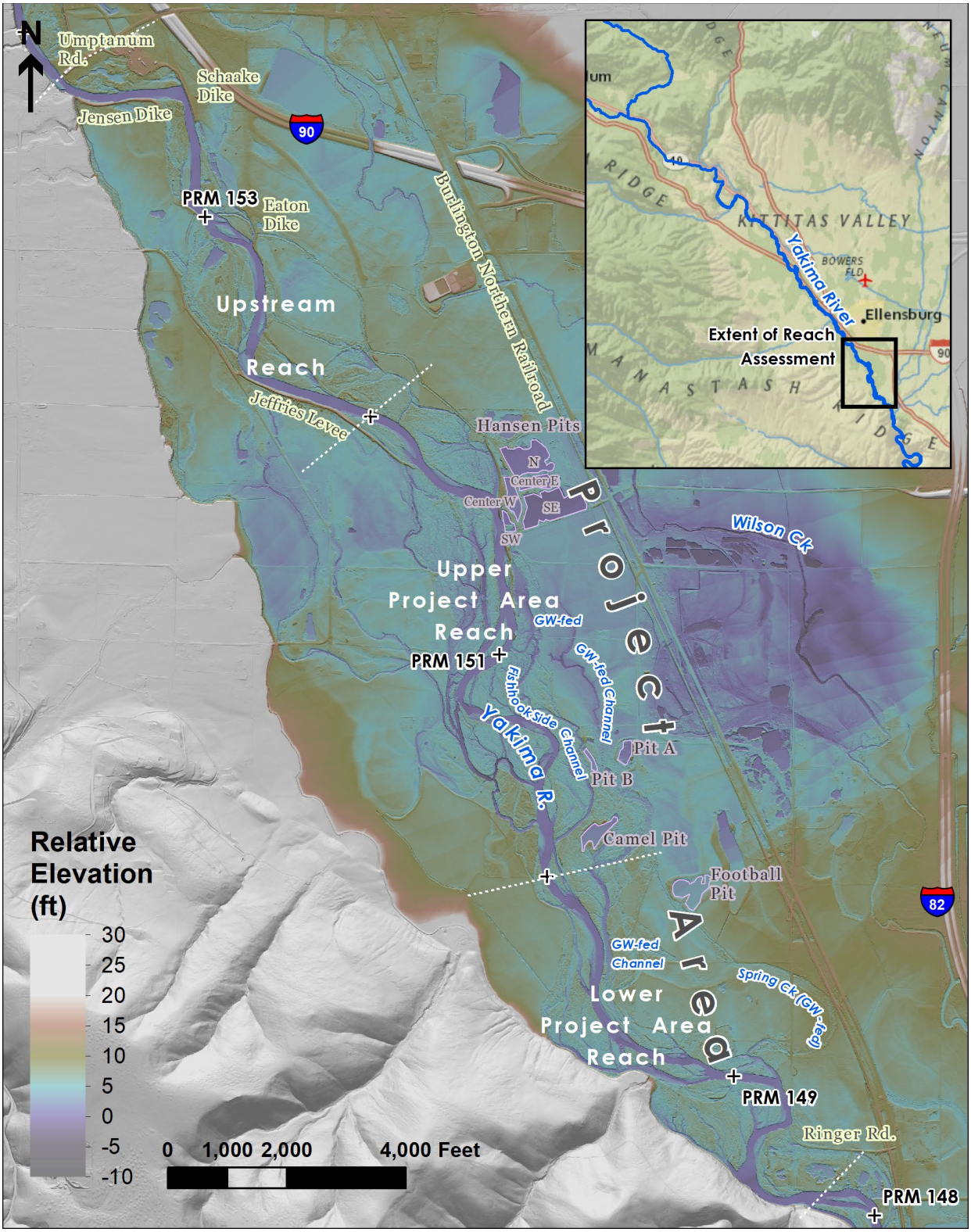

Figure 1.1: Relative Elevation Model of the Geomorphic Assessment Reach and Project Area.

2 FIELD OBSERVATIONS

NHC completed field assessment January 9 – 10, 2025. NHC staff conducted boat-based observations of the reach on January 9, 2025, to document existing bed material (including both qualitative characterization and collection of quantitative pebble counts), large woody material (LWM) abundance and function, and bank conditions. Staff floated and noted observations from Irene Reinhart Park near Umptanum Rd at project river mile (PRM) 153.8 to the Ringer Boat Ramp near PRM 148.2[1]. Weather conditions were overcast with air temperatures of approximately 32°F, and snow depths up to 6 inches. The extent of the active channel was generally snow-free. Yakima River flows during the field observations were near seasonal low flows, reported as approximately 1,000 cfs at the Yakima River at Umtanum gage (12484500). On January 10, 2025, staff conducted site walks along select areas of the project area and adjacent floodplain (focused near PRM 149, PRM 150-151. And near PRM 151.5) to further observe gravel pits and other geomorphic features of the proposed floodplain restoration. The following sections summarize field observations of the project reach, broken into three sub-reaches of similar geomorphic character.

PRM 153.8 to 152 – Upstream of Project Area

The first sub-reach extends from PRM 153.8 near Umptanum Rd/Irene Reinhardt Park downstream to PRM 152. This sub-reach is confined by terraces (Photo 2.1), levees, and rock revetments (Photo 2.2) for most of the channel length, which confine the channel (about 65% confinement following the definition of Fryirs et al., 2016) resulting in active channel widths in the range of 175 to 300 feet, which are narrower than the downstream reaches. Many revetments in this sub-reach were in poor condition, with five of seven observed revetments showing signs of failure. Unstable and partially stable bank conditions were observed along portions of the bank that were not protected by revetments. One area of partially stabilized bank near PRM 152.3 was stabilized by roots of mature (30-40 year) cottonwood trees.

Connections of the mainstem channel to side channels and groundwater fed springs are relatively infrequent in this sub-reach compared to other sub-reaches due to the presence of confining levees and revetments. Functional large wood) that forces geomorphic process and channel complexity is notably absent for most of the channel length. Bed material in this reach is primarily cobble to gravel-sized, with some areas of finer gravel present. The pebble count collected from this reach (PC1) was the coarsest of the five pebble count observations (Figure 2.1). The channel in this sub-reach is typically single-thread, and the presence of exposed gravel bars is notably less frequent in this sub-reach compared to the other sub-reaches downstream. One exception is near PRM 153, where the active channel is wider than typical (approximately

[1] Project river miles were updated from USGS River Miles by setting PRM 146 identical to USGS RM 146 and then recalculating the river miles along the 2020 channel centerline delineated from the LiDAR upstream of this point.

600 feet), with branched flow around multiple gravel bars composed of cobble to fine gravel. Multiple accumulations of functional LWM are present on the gravel bars near PRM 153 and downstream (See Appendix A, Sheet 1).

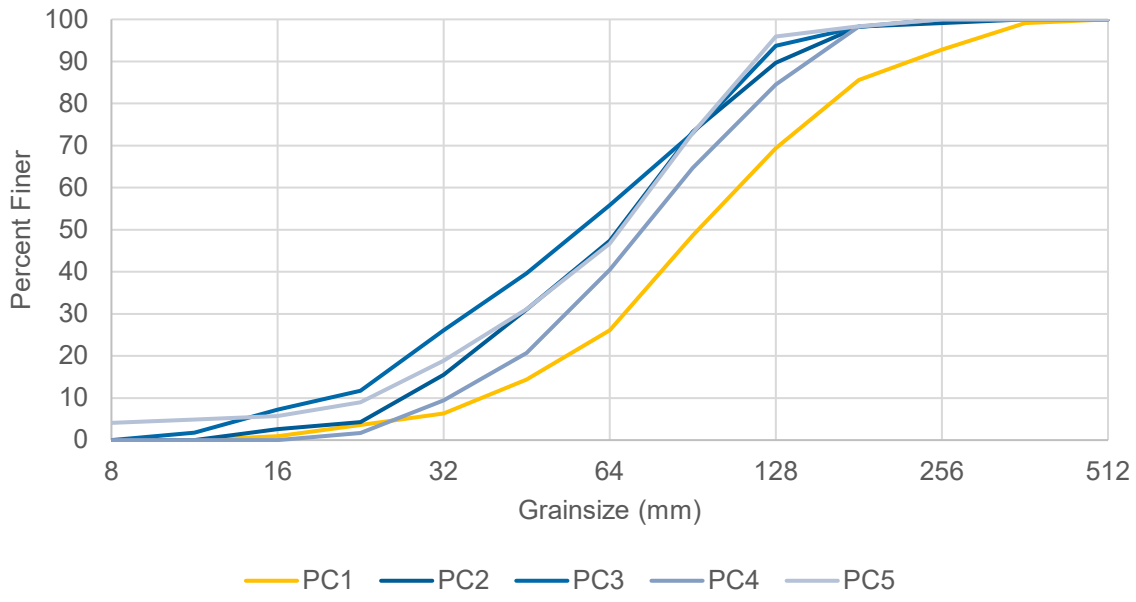

Figure 2.1: Cumulative Grain size Distribution Curves for Pebble Count Observations

Active erosion on the right bank at PRM 153 is currently about 150 ft from a 1.3-acre floodplain pond that lies along a preferential avulsion path for the river. Review of aerial photos shows a connection between this pit and the channel upstream has formed and filled with LWM repeatedly since 2009 and avulsion through this pit is likely in the future. This would likely result in a substantial realignment of the river, which may result in changes in the interaction between the channel and the Jeffries Levee just downstream. The Jeffries Levee currently confines the channel on river right from PRM 152.4 to 152.1 and directs flow of the mainstem towards the Hansen Dike on river-left at PRM 151.4 to 151.5.

Photo 2.1: Looking at the right bank, upstream towards the Umptanum Rd. bridge near PRM 153.8. Steep vertical banks and fresh slumping were observed immediately downstream of the bridge.

Photo 2.2: Looking downstream from PRM 153.7 towards the failing revetment (Jensen Dike) on the right bank.

PRM 152 to 150 – Upper Portion of Project Area

This sub-reach extends from PRM 152 upstream of the Hansen pits downstream to PRM 150 and is noticeably less confined than the sub-reach upstream. The Hansen gravel pits occupy a

portion of the river left floodplain between PRM 151.4 -151.8. Fewer levees and bank revetments, compared to the upstream sub-reach, allow for a wider active channel belt—approximately 1,500 feet in width—with a predominantly multi-threaded planform supporting two to four anabranches (See Appendix A, Sheet 2). Frequent occurrences of vegetated bars and islands contribute to greater habitat complexity compared to the more constrained conditions observed in the upstream sub-reach.

Bed composition in this sub-reach is primarily cobble to gravel-sized material, and generally finer than the upstream sub-reach (Photo 2.3). Functional LWM accumulations occur more frequently than in the upstream sub-reach, likely due to lower confinement (as described in later sections). The large wood is mostly present as bank jams where overbank flows leave the channel and localized apex and flow deflection jams, some of which appear to have been constructed. These LWM accumulations—both natural and constructed—generally do not have a strong influence on channel morphology.

There are multiple side channels, some of which form 2nd order side channels and groundwater-fed tributaries through this sub-reach. These likely provide high quality salmonid rearing habitat and thermal refugia. There are fewer areas of unstable bank within this sub-reach compared to other observed subreaches in the project area; those that were present tended to coincide with locations of active channel migration and wood recruitment (Photo 2.4).

The river has eroded through the downstream portion of the Hansen Dike at PRM 151.5 and has connected to the Hansen floodplain pit closest to the river (Photo 2.5). This pit has mostly filled with fine sand and silt since it became connected to the river (Photo 2.6).

Photo 2.3: Looking east from PRM 150.4, near the location of PC3. In the background, the left bank is an area of active channel migration into mature cottonwood forest.

Photo 2.4: Looking south (downstream) towards a widening side-channel with spanning wood on right bank at PRM 150.8.

Photo 2.5: Near PRM 151.5 looking east towards the left bank and Hansen pits beyond. The breached section of levee can be seen in the center left of the photo.

Photo 2.6: Looking east from the left bank at PRM 151.5 towards the Hansen pits. The pit in the foreground has been breached (center right of photo) and is connected to the main channel.

RM 150 to 148.2– Lower Portion of Project Site to Ringer Boat Ramp

This sub-reach extends from PRM 150 downstream to PRM 148.2 near the Ringer Boat Ramp. It is partially confined with short and discontinuous flood berms (informal levees) and revetments (Photo 2.7). In the downstream portion of the reach, (RM 148.2-148.5) the right bank valley wall (Photo 2.8) confines flood flows and reduces lateral mobility, limiting the formation of avulsion-driven side channels. As a result, the channel in this sub-reach typically supports just one or two anabranches with an active channel belt of approximately 600 feet wide. Bed material in this sub reach primarily consists of cobble and gravel. LWM accumulations are frequent throughout the sub reach and are mostly apex jams and single key pieces, with one observation of a large meander jam at a point where flood flows enter a floodplain channel feature at PRM 149.4. Many groundwater-fed floodplain channels are connected and contribute to the mainstem through this sub-reach. Beaver activity and associated dam-building was observed in some of these floodplain channels (Photo 2.9).

Bank erosion is occurring near revetments and other confined segments. One area of notable bank erosion was near Ringer Road, where the entire roadway prism has been eroded by lateral channel migration (Photo 2.10).

Photo 2.7: Looking downstream along a side channel near PRM 148.9. The left bank of the side channel has rock spur revetments with LWM.

Photo 2.8: Looking south towards the right bank near PRM 148.6, the main channel is against the toe of the valley wall. The main channel is wide and shallow with abundant LWM.

Photo 2.9: Looking north from PRM 149.3 towards the left bank and the outlet of a groundwater-fed floodplain channel. Beaver activity was observed upstream in the side-channel.

Photo 2.10: Looking east toward the right bank from PRM 148.8 at the Ringer Rd washout. Dark material in center left of photo is fill from the road embankment.

Floodplain Observations

NHC staff accessed portions of the left bank floodplain on foot to observe geomorphic features, floodplain and smaller side channels, and surface indications of groundwater activity. We observed large areas where agricultural grading had reduced floodplain relief (Photo 2.11). However in areas of low topography, which include modified relict channels and may include constructed ditches, there were abundant indications of seasonal shallow groundwater emerging from springs (demonstrated by rapid longitudinal changes in discharge) into these channels(Photo 2.12). These groundwater-fed flow paths appear to create a complex network of small (a few feet wide) to moderately sized (tens of feet wide) floodplain channels, which we did not trace out in detail in the field. Some of these included indications of ongoing beaver modification.

Photo 2.11 - Broad floodplain (left) downstream of Hansen pits (right), looking west the SE corner of the SE pit towards the river near PRM 151.4

Photo 2.12 – Looking upstream at a groundwater-fed side channel that contributes flow to the "Fishhook" side channel, near PRM 150.5.

3 RIVER PROCESSES

This section outlines key interactions among the historical flood flows, hydraulics through the project area, sediment transport, and channel-forming processes. The section incorporates information from both review of relevant literature, referenced throughout, desktop geomorphic analysis informed by the field observations.

3.1 Hydrology and Flood History

The USBR (USBR, 2024) Concept Basis of Design Report for the project area includes a hydrologic analysis that integrates previous work in the project area. The Flood frequency (return interval) discharge estimates provided by USBR are specified in Table 3.1.

It is also important to understand the flood history when interpreting observed geomorphic conditions. Thes are documented here to provide background for that interpretation, which follows in later sections Annual peak flows over the last decade have been below average. Recent notable flood events occurred in 2011 (~10-yr return interval), 2009 (~20-yr), and 1996 (~ 50-yr). Figure 3.1 shows annual maximum floods for the period of record (1911-present) and the cumulative deviation in those flood peaks through time. The cumulative deviation plot is calculated by serially adding the difference between each year's flood peak and the long-term average. The slope of the line shows how conditions over shorter periods relate to the long-term average with positive slopes indicating periods with higher-than-average flood peaks and negative slopes indicating periods with lower-than average flood peaks. Though there have been notable large floods over the past several decades, the negative slope of the line shows peak flows have been lower than the average for the period of record.

Table 3.1: Design discharges, sources, and descriptions. From USBR (2024)

Name or Return Interval in Years	Discharge (cfs)	Source	Description/Comment
Low Habitat Flow	700	CH2M, 2016	Used to set the lowest flow when side channels were to connect and initiate flow on Schaake.
1.01	2,640	CH2M, 2016	Discharge with the least amount of juvenile salmonid habitat availability (Reclamation 2008).
Summer Irrigation Flow	3,500	CH2M, 2016	Occurs for an extended time during the growing season.
High Irrigation Flow	4,200	Reclamation	High end of what can occur for an extended time during the growing season.
1.25*	4,800	Reclamation, 2019	Low-end of bankfull discharge possibility.
1.5	6,000	Reclamation, 2019	Design discharge used to set overtopping (i.e., designed bankfull discharge).
2	7,170	CH2M, 2016	Expect minor flooding
10	14,000	CH2M, 2016	Expect major flooding
20*	17,400	CH2M, 2016	
50*	22,800	CH2M, 2016	
100	32,300	FEMA, 1981	Large-scale flooding
500*	43,600	FEMA, 1981	

Flood peaks and flow duration have an important relationship with channel formation and sediment transport. Figure 3.2 shows flow duration curve for the Umtanum gage and scaled flows to the project site about eight miles upstream of the gage. Flows were scaled to the project site based on an Area-Transposition scaling factor of 0.76 (Sumioka et al., 1998).

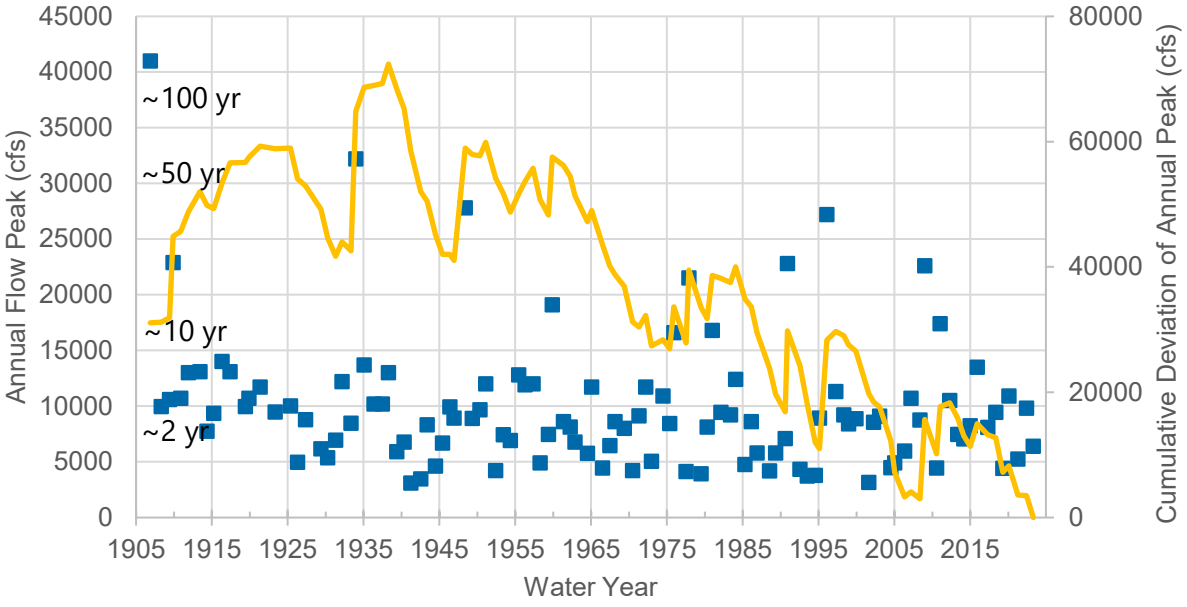

Figure 3.1: Annual Peak Flow History for Yakima R. at Umtanum (USGS Gage 12484500). Approximate recurrence intervals indicated are 20% higher than the USBR design flows for the project site to account for the additional contributing area at the gage.

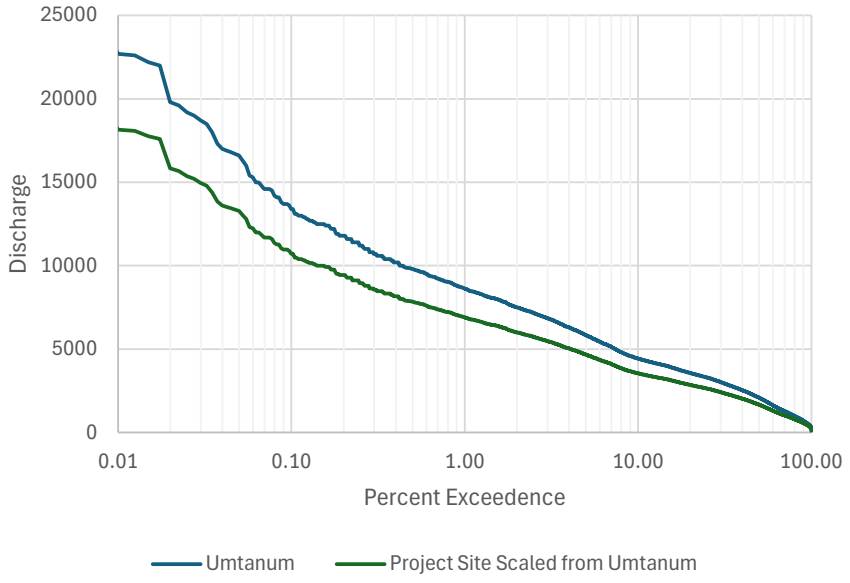

Figure 3.2: Flow duration curve for Umtanum Gage (USGS Gage 12484500) with scaled duration curve at the project site.

3.2 Hydraulics and Sediment Mobility Overview

NHC conducted a quantitative analysis of river conditions using the observations presented above coupled with computed 2D numerical model results provided by Inter-Fluve[2]. Figure 3.3 shows how variability in the channel depth and slope (bottom panel) affect shear stress, a measure of the force available on the channel boundary (second panel above the bottom) to mobilize bed material (top two panels). The top panel shows the pebble count results, interpolation between them and estimates of the excess shear expressed as the ratio between the shear stress and critical shear stress required to mobilize the bed material. Values below 1 indicate little to no mobility of the bed, values close to 1 the beginning of bed mobilization, and values above 1 indicate a relatively mobile bed. Despite higher shear stresses in the upstream portion of the assessment area (RM 152.5), larger bed material results in lower material mobility in this area—suggesting it is a transport reach, through which gravel-sized material gets flushed into the middle (RM 150-152) reach.

In the middle reach (RM 150-152), thalweg shear stresses are generally large enough to mobilize small cobble during flows exceeding the 1.5-yr estimated discharge (6,000 cfs) flood flow (see section 3.1 for a summary of reach hydrology). Although the shear stress in this reach is moderate, the presence of smaller grain sizes (which have relatively low critical shear stress) results in the highest excess thalweg shear stress (T/T_c) and interpreted relative bed mobility within the modeled reach.

Shear stress declines in the downstream-most reach (RMn148-150) and the bed material in this reach is relatively gravelly compared to the upstream reaches with about equal dominance of cobble and gravel on bars. Overall, the general pattern of a downstream decrease in slope and shear stress suggests the project reach has lower capacity to export sediment than the upstream reach. This combination of conditions likely favors equilibrium or slightly aggregational channel profile adjustment patterns and drives the upstream-to-downstream reduction in the bed material grainsize.

[2] From the U.S. Bureau of Reclamation's (USBR) 2D HEC-RAS model

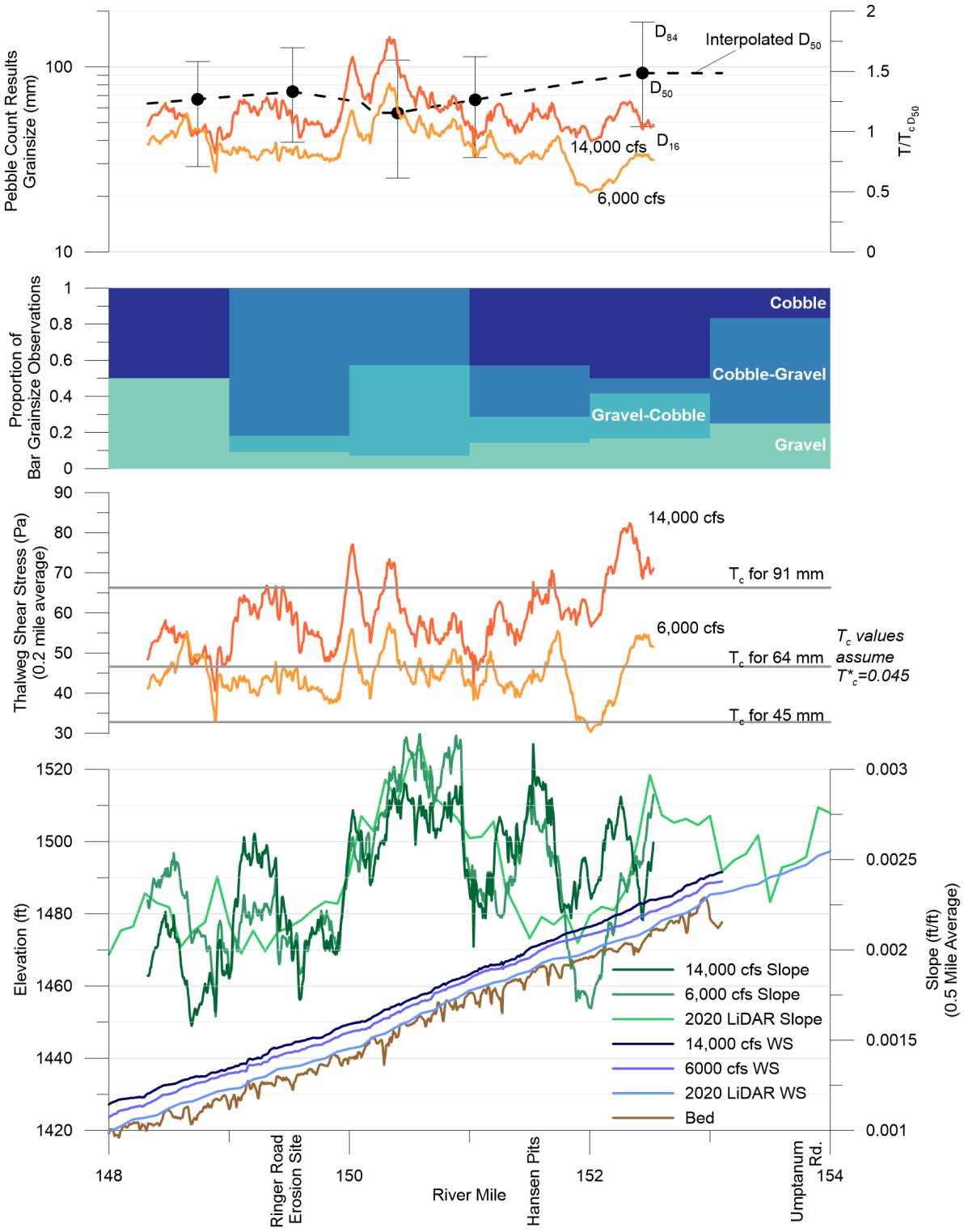

Figure 3.3: Relation of hydraulics (extracted from USBR 2D HEC-RAS Model; bottom two panels) and grainsize information from field observations (top two panels) to evaluate relative patterns of sediment mobility through the project area (top panel).

3.3 Sediment Transport

Bed material transport measurements were collected and calibrated modeling completed on the Yakima River just above the confluence with the Naches River (30 miles downstream of the project area) by (Hilldale and Godaire, 2010). At the downstream location, the total basin area is about 1.8 times larger than at the project site and the sediment contributing area is about 2.2 times larger than at the project site due to influences of lakes in the Yakima River headwaters. Although it is somewhat distant from the project site, this location provides important information because calibration observations are available reducing uncertainty in the bedload transport calculations by an order of magnitude compared to application of an uncalibrated hydraulics-based bedload transport function. Based on their analysis, the Yakima River transports on the order of 25,000 tons per year of bed material load[3] past the USGS Selah gage (12487000) just above the Naches River confluence, with about half of that being suspended sand transport and about half bed load transport. If the same sediment yield per unit area (specific sediment yield) is assumed for upstream of the project site and the area between the project site and Naches River confluence, then this gives an estimate of about 11,000 tons per year that would be predicted for the project site. This is calculated by transposing the 25,000 tons per year of bed material load value from Hilldale and Godaire's analysis downstream, considering the difference between the sediment contributing area at the two sites (799 mi^2 for the project area and 1,739 mi^2 for the Yakima River just above the Naches confluence). Specific sediment yield varies widely across the landscape, and so this provides only a rough estimate.

As part of this assessment, bedload transport potential at the project site was evaluated by applying the BAGS sediment transport software (Pitlick et al., 2009). This application used channel geometry from the USBR concept design existing conditions model, grainsize distributions at the PC 2 (RM 151) and PC 5 (RM 148.) pebble count locations, and project site scaled flow duration curves shown in Figure 3.2. This analysis, summarized in Figure 3.4, indicates that potential bedload transport at the project area is on the order of 2,000 ± 1,000 tons per year. Assuming the same ratio of bedload to bed material load identified by Hilldale and Godaire (2010), this would equate to 2,000 to 6,000 tons per year of bed material load transport through the project area. The bed material load calculated here is comparable to but lower than the value of about 11,000 tons per year that would be predicted for the site by scaling the results of Hilldale and Godaire.

[3] Sediment transport in rivers can occur through a variety of mechanisms and different grainsizes play different roles in the geomorphology of the river and valley bottom. Because of this, it is important to use somewhat precise vocabulary when talking about different material types. **Bed material** represents the grainsizes that are dominant in the bed and bars of the river and includes gravel, cobble, and some of the sand transported by the river. **Wash material** is comprised of silt, clay, and some of the sand transported by the river and generally forms the upper portion of floodplain deposits. Wash material is transported in suspension, while bed material can be both transported in suspension and through saltation and traction. See Church (2006) for a through description of these relationships.

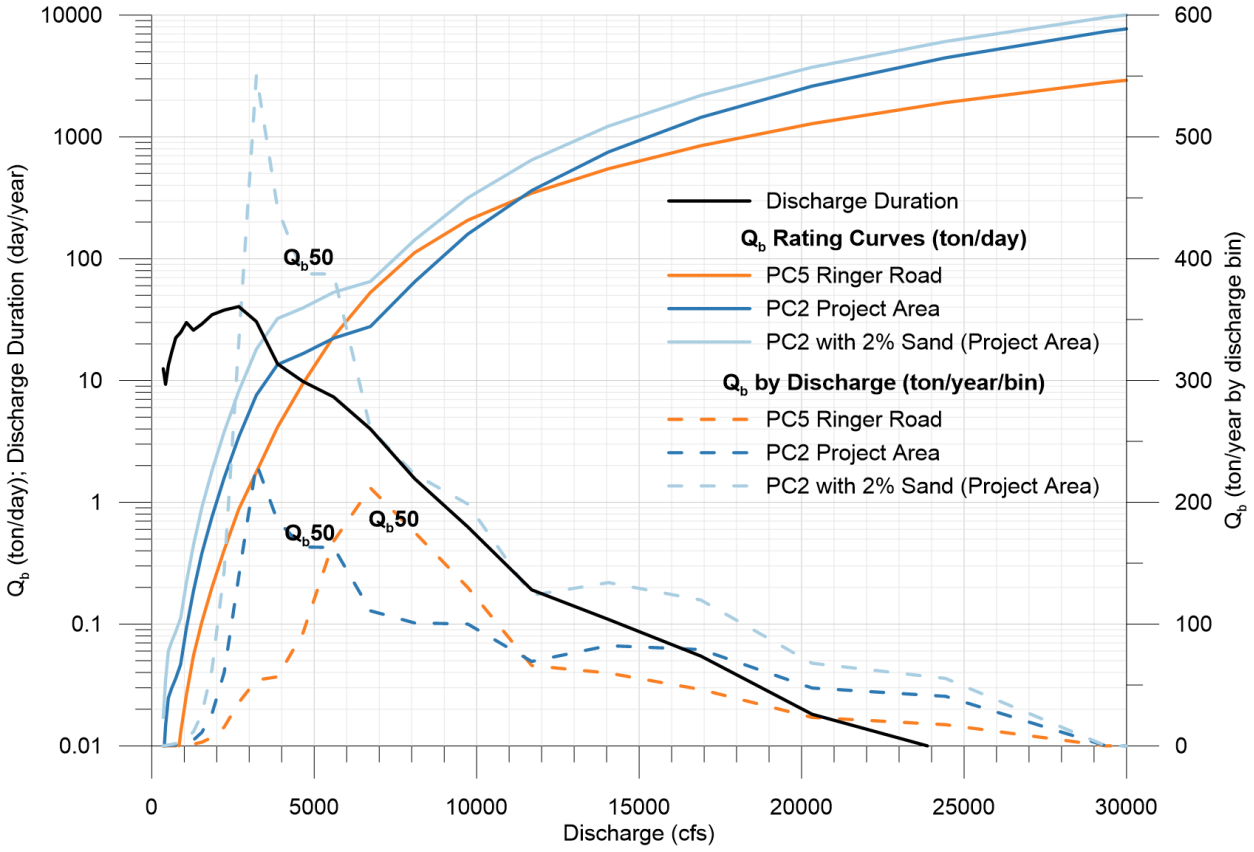

Figure 3.4: Bedload Transport Rate (Q_b) at PC2 and PC 5 sediment sample locations shown as a function of instantaneous discharge and weighted by the duration of that discharge. Results for PC2 show values with and without 2% sand added to the field-based pebble count result showing sensitivity of the function to that parameter, which is not precisely known. Q_b50 indicates the discharge above and below which 50% of bedload transport occurs based on the rating curves and flow durations used.

NHC has not been able to identify long-term suspended sediment transport or yield information for the Yakima River in proximity to the project area. USGS data (Anderson et al., 2023) from the Kiona gage (USGS 12510500) on the Yakima River at USGS RM 30, which has a total contributing area of about 5,615 mi^2 and a sediment contributing area of about 4,966 mi^2 indicate that the total suspended sediment transport yield there was about 100,000 tons per year for the period from June 2018 through June 2022. This was composed of about 88 percent fines (silt and finer) and 12 percent sand. Scaling this to the subject reach, which has a sediment contributing area of 799 mi^2 introduces considerable uncertainty because of the large difference in contributing area as well as the physiographic differences of the contributing basins. Despite these differences, the comparison provides one perspective on the suspended sand to bedload assumptions described above and gives a sense of the order of magnitude of wash load (silt and clay) transport. This exercise suggests the suspended sand yield supplied to the subject reach may be on the order of 2,000 tons per year and the suspended fine yield on the order of 14,000 tons per year. This is

a very low unit sediment yield compared to the contributing basin area compared to typical regional values (Church and Slaymaker, 1989; Nelson, 1973).

Total potential sediment transport and the fraction that is bedload, suspended sand load, and wash load can be estimated by combining the values identified above. A monte-carlo (n=2,000) analysis was completed to evaluate the range of combined uncertainty. This analysis assumed 33% uncertainty (±1σ) in the suspended sand and wash load estimates scaled from the Kiona gage and 50% uncertainty in the BAGS-based bedload transport estimate (±1σ) with a minimum plausible average annual transport threshold of 100 tons applied. Results of this analysis are summarized in Table 3.2.

All grain sizes transported by the river may infill connected floodplain pits. For the purposes of understanding the potential infilling rate, we assume that the bedload and suspended sand load combined is the bed material load of 4,200 ± 1,800 tons per year and that this material will dominate sedimentation in any connected pits. We assume a typical bulk density of 1.3 tons per cubic yard to give a volumetric annual bed material load transport rate on the order of 3,200 ± 1,400 cubic yards. This estimate is combined with documentation of the pit geometry to evaluate expected durations to fill the pits in for the different scenarios in Section 4.2 of this report.

Table 3.2 Summary of Monte-Carlo Total Sediment Yield Analysis Relating BAGS bedload estimates in the subject reach and USGS suspended sediment measurement scaled to the contributing basin to estimate overall uncertainty in total load.

Sediment Transport Component	Estimate (tons/year)	Uncertainty (±1σ)	Fraction of Total Load	Fraction uncertainty (±1σ)
Bedload	2,100	1,200	0.12	0.08
Suspended Sand Load	2,000	700	0.12	0.06
Wash Load (suspended silt and clay)	14,100	4,600	0.76	0.10
Total Load	18,200	4,900	1.00	

3.4 Channel Migration and Historic Channel Patterns

Watershed Science and Engineering completed an evaluation of channel migration processes and hazards in the project area (WSE, 2021). Their assessment identified that regulated peak flows and a shift in the timing of peak flows, bank armoring, and flood protection along the Yakima have reduced lateral channel migration and the frequency of avulsions, which have also reduced the flux and storage of large wood in the river. They found long-term channel migration rates of actively eroding meander bends range from 3 to 7 feet per year and that short-term migration rates can exceed 40 feet per year (Figure 3.5). Based on this analysis, they concluded that migration buffer of 340 feet along the mainstem of the Yakima River would encompass expected migration through gradual meander processes over a 50 year period, but that there is a large avulsion hazard zone formed by the network of floodplain side channels that span much of the valley bottom. They also observed that partial avulsions are a common side-channel forming mechanism, especially within large meander bends.

WSE evaluated the likely short-term response of the river to removal of the revetment and levee between the Hansen Pits and the river. They expect that within ten years this would result in acceleration of eastward migration of the meander currently adjacent to the pits, resulting in engagement of the downstream margins of the three southwestern pits.

For this project, NHC completed a rough analysis (channel delineation scale of approximately 1:4,000) of historical channel migration and occupancy (Figure 3.6). This analysis highlights the large effect levees, revetments, and associated channel straightening have had on reducing lateral channel migration and anabranching intensity. It also highlights that the anabranches and islands through the project area have persisted through time.

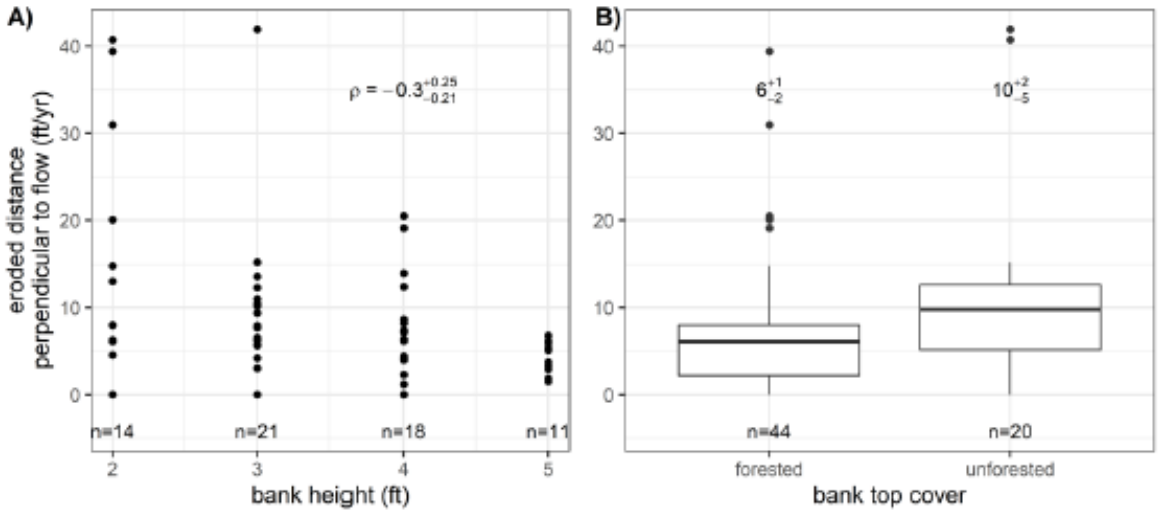

Figure 3.5: Control on variable meander migration rates in the subject reach of the Yakima River. From WSE (2021).

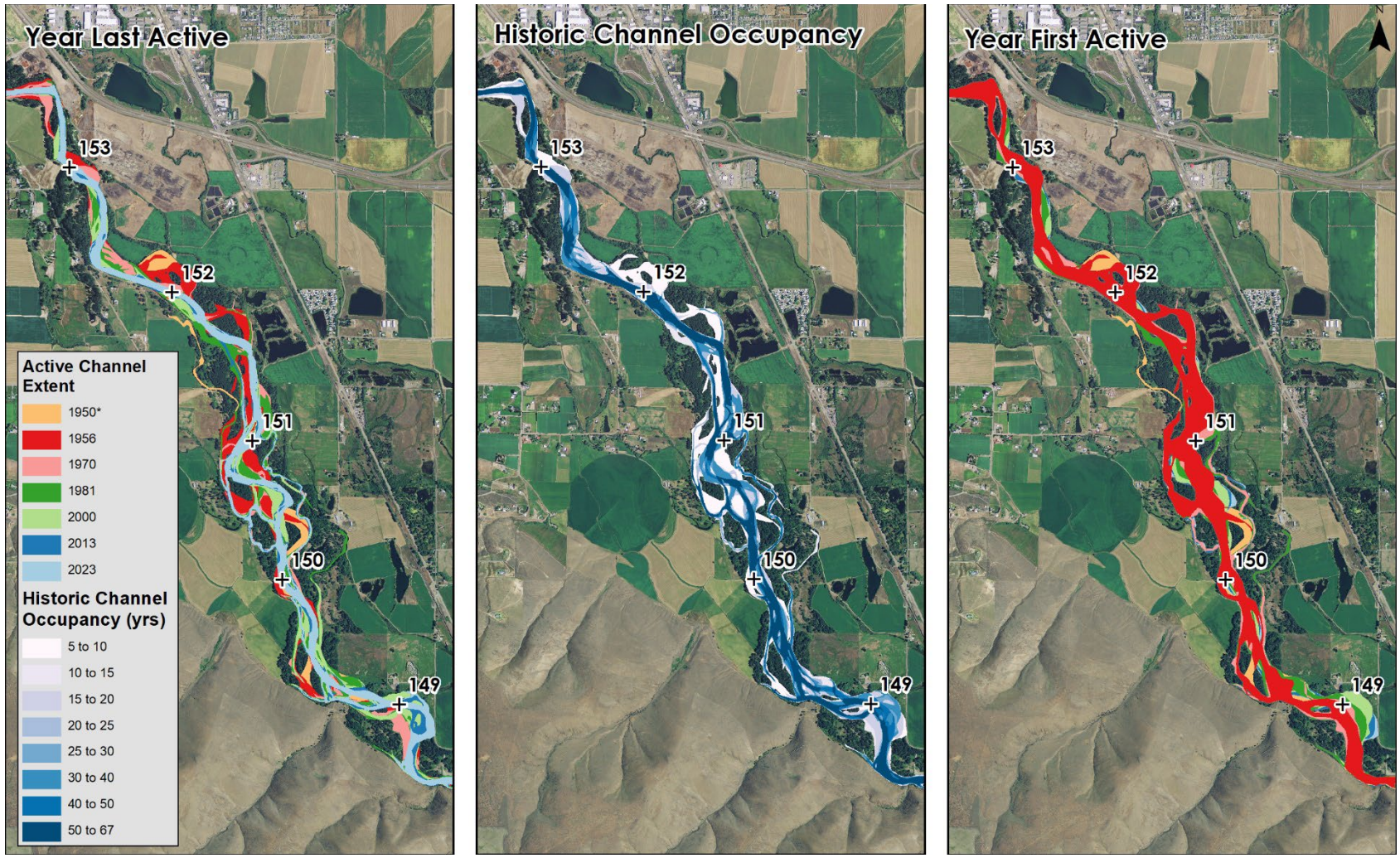

Figure 3.6: Historical Yakima River positions and channel occupancy from NHC bank line mapping. Note areas mapped as being active channel in 1950 were observed to have been recently abandoned by the river in 1956. The actual last date of activity for these locations is unknown. The year last active panel (left) draws the layers from youngest to oldest and highlights the timing of floodplain formation. The year first active (within the analysis period) panel (right) highlights areas and patterns of floodplain erosion.

Long-term average erosion rates have been highest from PRM 150-152. (Table 2.3). These rates are somewhat lower than the individual meander migration rates documented by WSE (2021). Comparison of variation in the erosion rates through time (Figure 3.7) shows that erosion rates were anomalously high in the decade between 1970 and 1980, which had relatively high flood flows (Figure 3.1), and have been relatively low over the past two decades, which have had relatively low flood flows.

Table 3.3: Sub-reach average erosion rates as a function of period elapsed.

Erosion Duration	Average Erosion Rate (ft/yr)		
	RM 148-150	RM 150-152	RM 152-154
10 yr	4.8	6.0	5.5
20 yr	4.3	5.2	4.7
50 yr	3.6	4.2	3.6
100 yr	3.2	3.4	2.7

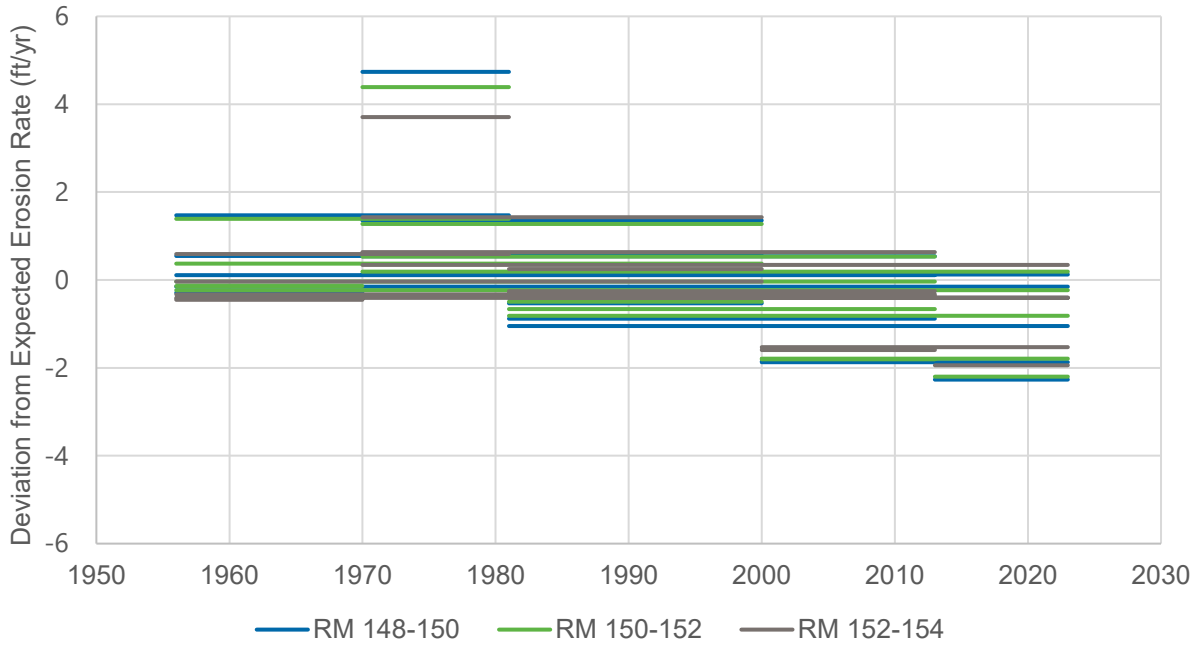

Figure 3.7: Deviation from expected migration rate for each elapsed period (e.g. Table 3.3) by observation period by analysis sub-reach.

A 1901 map of the subject reach (Figure 3.8) shows that the channel belt width had been substantially reduced by 1956 and that the reach supported 2 to 3 principal anabranches and a complex network of floodplain channels.

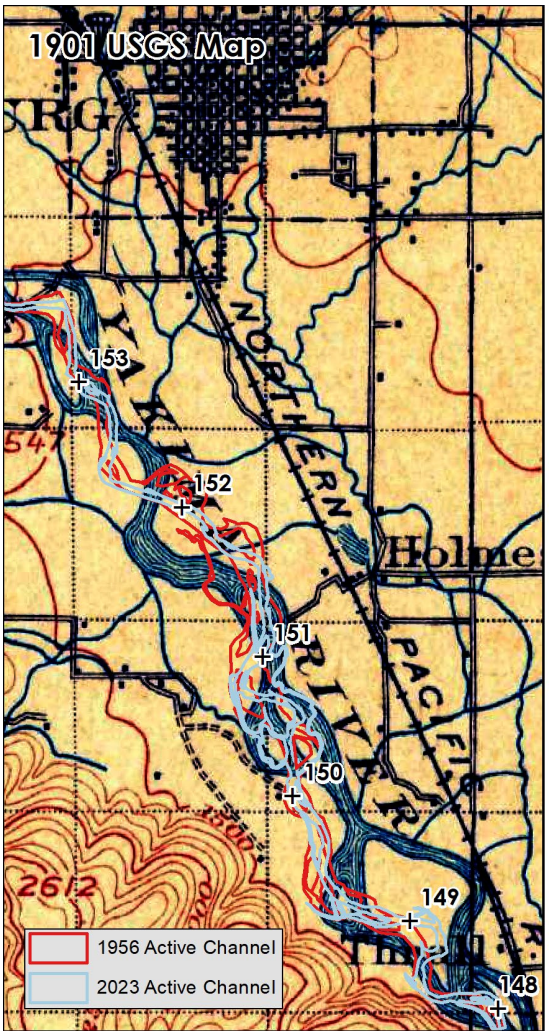

Figure 3.8: 1901 Map Illustrating Reach compared to 1956 and 2023 bank lines.

3.5 Floodplain Sedimentation

Floodplain sedimentation rates were evaluated by calculating the distribution of relative elevations across the floodplain, divided into zones by the period of most recent channel occupancy (Figure 3.6). To do this, a relative elevation model (REM) was constructed from 2020 LiDAR data characterizing the floodplain elevation relative to the water surface in that dataset. Polygons of floodplain age (Figure 3.6, left panel) (excluding areas isolated from the river by levees) were queried to extract the relative elevations present within each age class and then sorted into cumulative relative elevation exceedance plots by age class. This analysis shows that

floodplain sedimentation rates are relatively low. The 50th percentile elevation increased by about 0.8 feet (from relative elevation 3.2 to 4.0) from areas that had been abandoned for 40 years compared to areas that had been abandoned for 10 years and by only about half a foot more for areas that had been abandoned for about 70 years. These calculations are consistent with bank stratigraphy field observations and the dominance of gravel in test pit observations (GeoEngineers, 2025). The typical stratigraphy included 1 to 6 feet of fine sand and silt, interpreted to be deposited by a combination of overbank flooding and aeolian processes, over coarse alluvium similar to the riverbed material.

3.6 Channel Scaling

The relationship between formative discharge and channel width and depth (hydraulic geometry) was evaluated by a combination of empirical data extracted from the USBR existing conditions 2D HEC-RAS model and theoretical calculations calibrated to those observations.

The width, depth, and discharge during the 6,000 cfs bankfull flow as simulated within the USBR model were extracted from the model outputs at 62 locations in channels of varying scale within the portion of the subject reach covered by the model (the model domain, PRM 153 to 148.2). These data show typical power-law regime scaling of channel dimensions channel forming discharge (Figure 3.9). Power-law regressions on these data show width (w) and mean depth (h) show a power-law scaling relation with the near-Bankfull discharge conveyed in each channel (Q) as follows: $w=1.13Q^{0.58}$ and $h=1.0Q^{0.19}$. The width relation has a lower coefficient and higher and the average depth relation has a higher coefficient and lower exponent than classic regime relations (e.g. Stevens and Nordin, 1990).

Thes hydraulic geometry scaling pattern that emerged from these data was interpreted through the lens of rational regime theory. Rational regime theory provides a useful tool for examining the key factors controlling the channel planform and hydraulic geometry, understanding expected channel response to higher flows, as well as the potential flexibility in channel form due to natural variability in water and sediment supply and anthropogenic changes —including both historical and potential future management actions. It is a robust physical- based approach for predicting channel dimensions that has been validated against a large empirical dataset that more closely matches the empirical data for this reach than classing regime relations. The University of British Columbia Regime Model (UBCRM Eaton et al., 2004; Eaton, 2007a; Millar et al., 2014) is based on this approach and accounts for more of the key controlling variables than traditional empirical regime equations (which often only consider discharge) utilizing readily determinable input parameters, described below. UBCRM is a physically based rational regime model designed to predict the equilibrium form of alluvial channels (Eaton and Millar, 2017). It represents an attempt to use a physically based approach to predict the configuration of stable channels that can transport the imposed sediment supply with the available discharge (Eaton and Millar, 2017).

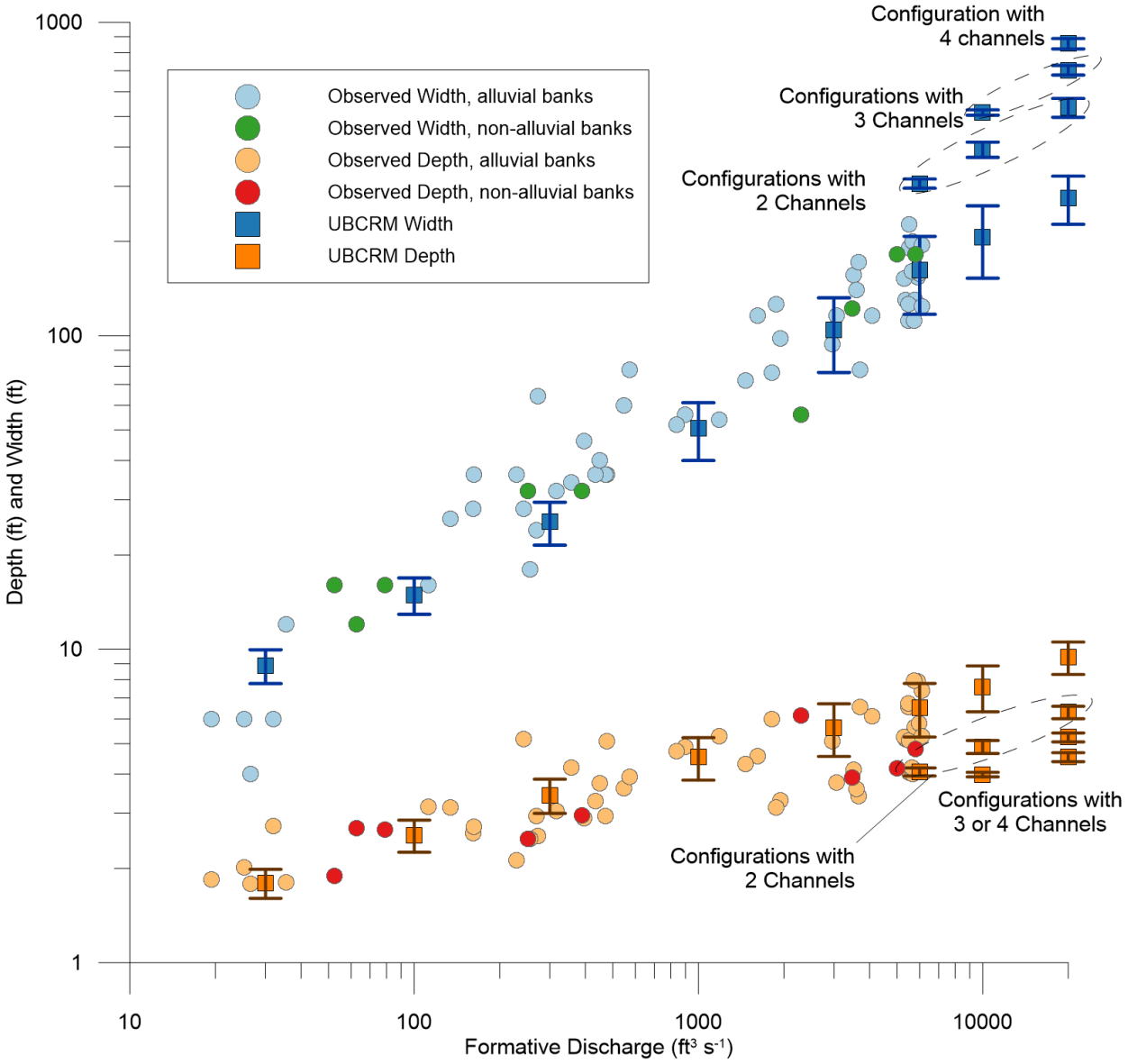

Figure 3.9: Regime relationships from empirical data and rational regime theory (UBCRM) evaluation extracted from across the model domain. Empirical observations are divided between locations with alluvial bank material and locations adjacent to revetment or bedrock banks. Error Bars on UBCRM results indicate the ±1σ range from the Monte-Carlo uncertainty analysis.

At its core, UBCRM seeks to find the most stable channel configuration (Eaton, 2006). It does this by applying physically based equations for flow hydraulics, bed material sediment transport capacity, and critically, bank stability and channel pattern stability(Eaton and Millar, 2017). Unlike simpler empirical regime equations that might only consider discharge1, UBCRM incorporates a broader set of key controlling variables, including formative discharge (Q), reach slope (S), bed material sizes (D50 and D84), and a bank strength parameter (μ or H) (Eaton, 2007b).

The model analyzes an idealized channel cross-section, which is either a simple trapezoid or a compound shape considering a stable upper bank. The dimensions of this idealized section (width, depth, bank angle) are iteratively varied to find a stable solution (Eaton, 2006; Eaton et al., 2004; Eaton and Millar, 2017). This stable solution is typically found by maximizing the dimensionless sediment transport efficiency for a given channel gradient, which is conceptually equivalent to minimizing the channel slope required to transport the sediment supply (Eaton, 2006; Eaton and Millar, 2017).

A crucial and unique aspect of UBCRM is that this efficiency maximization is constrained by the requirement for stable channel banks3.... The bank stability analysis is based on the conceptual model that the primary effect of vegetation is to create a stable upper bank, with the bank's overall position determined by the erosion of unvegetated bed material at the toe (Davidson and Eaton, 2018; Eaton, 2006). Bank strength can be represented using a parameter (μ or H) that integrates effects of grain size, cohesion, and vegetation roots. Erosion at the bank toe, which can control the retreat rate even with a cohesive upper layer, is assumed to occur when the D84 of the bank toe material is fully mobilized (Davidson and Eaton, 2018).

Furthermore, UBCRM also seeks the most stable channel pattern. It includes a simple braid criterion based on the principle that wide, shallow channels tend to develop mid-channel bars, which can lead to multi-threaded or anabranching patterns(Eaton et al., 2010; Eaton and Millar, 2017). The model predicts the number and average size of these stable anabranches, distinguishing this stable, divided pattern from unstable braided channels (Eaton et al., 2010). Because of its strong control over width to depth ratios in the model, channel the channel pattern predicted by the model is also linked to relative bank strength.

Like all regime models, UBCRM is fundamentally based on the assumption that the river system is at grade (Eaton et al., 2010; Eaton and Millar, 2017). This means the channel configuration is adjusted to efficiently pass the imposed sediment supply with the available discharge over the long term. The model is best applied to reaches that are at least 5 to 10 channel widths in length and exhibit relatively consistent geometry. It assumes that primary flow resistance is determined mainly by bed grain size, and that there is significant bedload transport. It's important to recognize that UBCRM is designed to predict response to persistent, long-term changes and does not explicitly model transient responses, short-term sediment pulses, or processes like aggradation, degradation, or avulsions that can drive a system far from a graded state in the short term.

The UBCRM application in this study utilized the specific values for formative discharge (Q), slope (S), D_{50}, D_{84}, and the critical Shields number for the bank toe (τ^*) shown in Table 3.4. All of these except the bank strength parameter (μ) are known. Reach slope was determined from the LiDAR water surface profile (Figure 3.3); the bed material values (D_{50} and D_{84}) were taken from field observations of the grainsize distributions (Figure 2.1); and the default value of τ^* of 0.02 for the bank toe material[4] was retained.

The bank strength parameter (μ) is defined as the ratio of the critical shear stress required to mobilize the bank material to the critical shear stress required to mobilize the D_{84} of the bed sediment. Bank strength integrates effects of the grainsize distribution, cohesion, and influence of vegetation roots, which increase the tensile strength of the bank soil. The value of μ is not quantitatively known, but the general observations of bank characteristics suggest it is typically low (slightly above 1) due to non-cohesive bank material and limited depth of riparian root stabilization. The model was calibrated to existing conditions by entering the known input parameters (listed in Table 2.4) and varying μ until the approximate observed active channel width was reproduced. This calibration procedure is a recommended approach (Eaton, 2015; personal communication) to evaluating conditions utilized in the model. The range of uncertainty in the model was evaluated by applying a Monte-Carlo analysis (n=400) for each discharge interval covering the uncertainty range specified in Table 3.4. Results of this analysis are shown in Figure 3.9.

Table 3.4 UBCRM Parameterization

Parameter	Value	Uncertainty Range
Formative Discharge (cfs)	Varied from 20 to 20,000 cfs	NA
Slope (ft/ft)	0.0025	±0.005
D_{50} (mm)	65	±10
D_{84} (mm)	114	±23
T*	0.02	0
μ	1.2	1.02-1.38

[4] τ^* for the bank toe material is typically much lower than for the general bed material and this parameter is normally not adjusted unless local empirical information is available.

3.7 Side Channel Formation

Comparison of the theoretical rational-regime theory based hydraulic geometry and empirical observations suggests that relatively infrequent larger floods are an important channel-forming mechanism. This is based on four principal observations:

1) A multi-channel planform is not predicted for any formative discharge less than 6,000 cfs, and even at 6,000 cfs formative (bankfull) discharge, only a small fraction (5%) of the Monte-Carlo results resulted in more than one channel. This indicates that in the project area, larger flood flows are needed to develop the anabranching planform that is locally dominant through the subject reach, as described in Section 2 and shown in Figure 3.6. UBCRM solutions for flows in the range of the 10- to 20-yr recurrence interval flood flow show anabranching morphologies become dominant for a formative flow between 10,000 and 20,000 cfs (Figure 3.10).

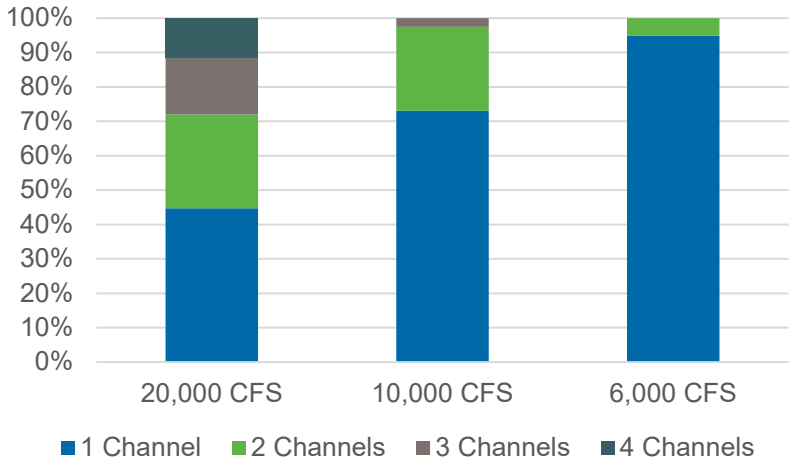

2)

Figure 3.10: Relationship between formative flow and number of channels predicted by UBCRM Mote Carlo analysis.

2) The recent channel history (Section 3.4) and an early map of the river under less confined conditions (Figure 3.8) show that a multi-thread planform is normative for the reach under unconfined conditions and that the channel can adopt a single-thread planform under higher confinement/bank strength conditions.
3) Individual channel threads consistently plot at or wider-than the theoretically predicted width for the discharge they presently convey during the bankfull flow. This is consistent with the interpretation above and suggests that side channel infilling are relatively low in the subject reach.

4) Apex jams are present at a relatively small fraction of bar and island features (37 and 22 percent observed in 2023 aerial imagery) and do not generally appear to be the primary mechanism leading to island or bar formation at those locations, even where present.

These conditions suggest that the river does not rapidly close side. This is likely due to a combination of low suspended sediment (Section 3.3) and altered high summertime irrigation discharge (Section 3.1), which is interpreted to supress establishment of vegetation in hydraulically-connected side channels. Groundwater-fed floodplain tributaries and seasonally extended high-water tables are also likely maintained as a result of the irrigation-altered seasonal hydrograph, relatively high porosity of the material the floodplain is composed of, and low overbank sedimentation rates. Restoration designs, therefore, may reasonably consider excavation of additional anabranch channels. The channel scaling relationships shown in Figure 3.9 can be used to guide the design of side channel dimensions.

4 RIVER FLOODPLAIN PIT INTERACTIONS

There are eight reasonably large floodplain pits within the project area, including the large cluster of six pits adjacent to the channel at PRM 151.5 called Hansen Pits (Figure 4.1) and a set of three smaller floodplain pits scattered across the floodplain between PRM 149.8 and 150.5 (Appendix A sheets 2 and 3). The size and general characteristics of the pits are provided in Table 4.1.

Table 4.1 Geometry of floodplain pits in the project area with potential to engage the Yakima River.

Pit Name	Area (acres)	Max Depth (ft)[a]	Mean Depth (ft)[a]	Volume (yd^3)[a]
Hansen North	7.6	11.6	4.2	52,000
Hansen SW	1.0	5.5	1.6	3,000
Hansen SE	9.9	19.1	10.3	165,000
Hansen Center W	2.6	10.9	6.9	29,000
Hansen Center E	2.6	11.6	7.1	30,000
A	1.5	NA	5.6[b]	13,000[b]
B	0.6	10.8	4.9	5,000
“Camel Pit”	3.0	NA	5.6[b]	27,000[b]
“Football Pit”	4.5	7.6	3.9	28,000

a) Pit Depth and Volume Estimates are below the low flow water surface based on topography in the USBR existing conditions hydraulic model terrain, unless otherwise specified.

b) Bathymetry of these pits was not specified in the model topography. The average of other pit depths is used to estimate the depths and volumes of these two pits.

Figure 4.1: Detail from Appendix A showing area of Hansen Pits and names for these used in the text. See Appendix A for full figure legend.

The possibility of river engagement of the pits described above poses both a suite of potential hazards as well as restoration opportunities. Principal hazards of this engagement related to geomorphic processes include:

- Rapid channel migration
- Avulsion through the pits and channel abandonment
- Upstream knickpoint migration and channel downcutting
- Downstream sediment starvation and channel downcutting

Potential restoration opportunities of the pits include:

- Increase riparian surface area
- Provide side channel or off-channel rearing area
- Increase channel complexity
- Spread flows (ranging from baseflow to larger floods) across a broad area of the floodplain.

Additional ecological and water quality considerations, such as predation on juvenile salmonids by warmwater fish resident in the ponds and rearing/refuge opportunities due to a different temperature regime in the ponds from the river are also likely important but are not the focus of this analysis. This section draws on previous work based on a review of channel response to eighteen floodplain pit connection events, including nine on the Yakima river (NHC, 2014; Nelson et al., 2015) to communicate and apply a framework for understanding the range of

plausible responses in the project area. It describes typical styles of river-floodplain pit engagement, defines some plausible "reference" engagement scenarios for the project area, and then applies a set of screening tools to evaluate the magnitude of each identified hazard. Finally, it considers what approaches may be used to mitigate the principal hazards.

4.1 Differentiating styles of river-floodplain pit engagement

As described by NHC (2014), two general types of processes are responsible for gravel pit capture by a channel: avulsion and lateral connection. Avulsions occur when the channel rapidly shifts course through the floodplain pit when a shorter, steeper, less obstructed path becomes available. An avulsion can either form a new side-channel, or it can cause a stream to completely abandon its previous course. The second type of capture is through lateral connection, which occurs when the channel migrates laterally, intercepts the perimeter of a pit, and widens locally but remains with essentially the same planform alignment.

Figure 4.2 illustrates key elements of channel response to an avulsion through a floodplain pit. Prior to pit capture, at time t0, the meander bend in the channel forms a relatively long path around the pit. A flood overflow or channel migration breaches the levee separating the upstream portion of the pit from the channel, allowing water to flow through the shorter, steeper path (t1). With a nearly flat-water surface profile, the pit causes the water surface in the upstream portion of the overflow path to become locally steeper. This over-steepening of the water surface creates very high shear stress on the bed, which causes a headcut to form and the bed upstream of the pit to erode (t2). In a coarse gravel bed river, the reach recovers (t3) when the upstream propagation of the headcut is halted by bed coarsening, bedload supply, or intersection with an existing grade control feature, such as a coarse riffle. The pit captures the bedload supply moving downstream and forms a delta that progrades across the floodplain pit until a stable bed slope and channel cross-section reform through the pit. At this point, the bedload supply is restored to the downstream reach.

Figure 4.3 illustrates the key elements of a channel's response to a lateral connection with a floodplain pit. In this case, the floodplain pit is often outside of the channel's meander belt (t0). Lateral channel migration intersects the pit (t1), which causes the channel to become oversized relative to a *regime channel*, which would be wider, deeper, or both and would reduce the local shear stress. A large bar develops on the inside of the meander bend, directing the flow into the former pit area where suspended sediment may be deposited in slack-water areas, and the channel thalweg migrates across the pit's area (t2). Headcut effects and bedload starvation may both occur, but the impacts are typically much more limited with a lateral connection than with an avulsion through a pit. As a point bar rapidly grows, channel lengthening offsets effective shortening by the pond, thereby limiting the headcut magnitude. Bedload starvation downstream is limited because bedload conveyance is usually partially maintained across the bar and because rapid channel migration often causes substantial floodplain erosion on the downstream side of the pond.

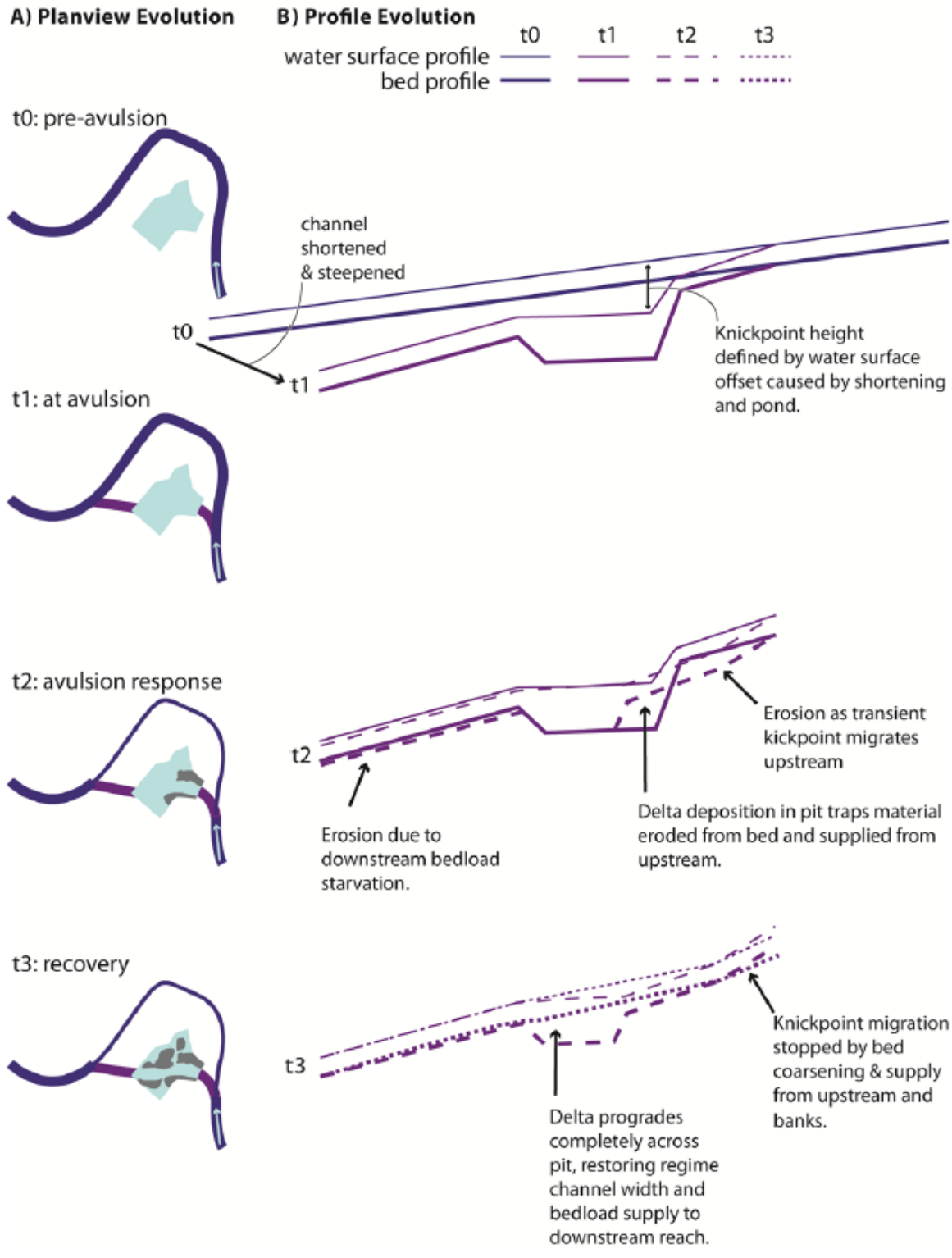

Figure 4.2 Schematic Illustration of plan view and profile response to an avulsion through a floodplain pit, from NHC (2014).

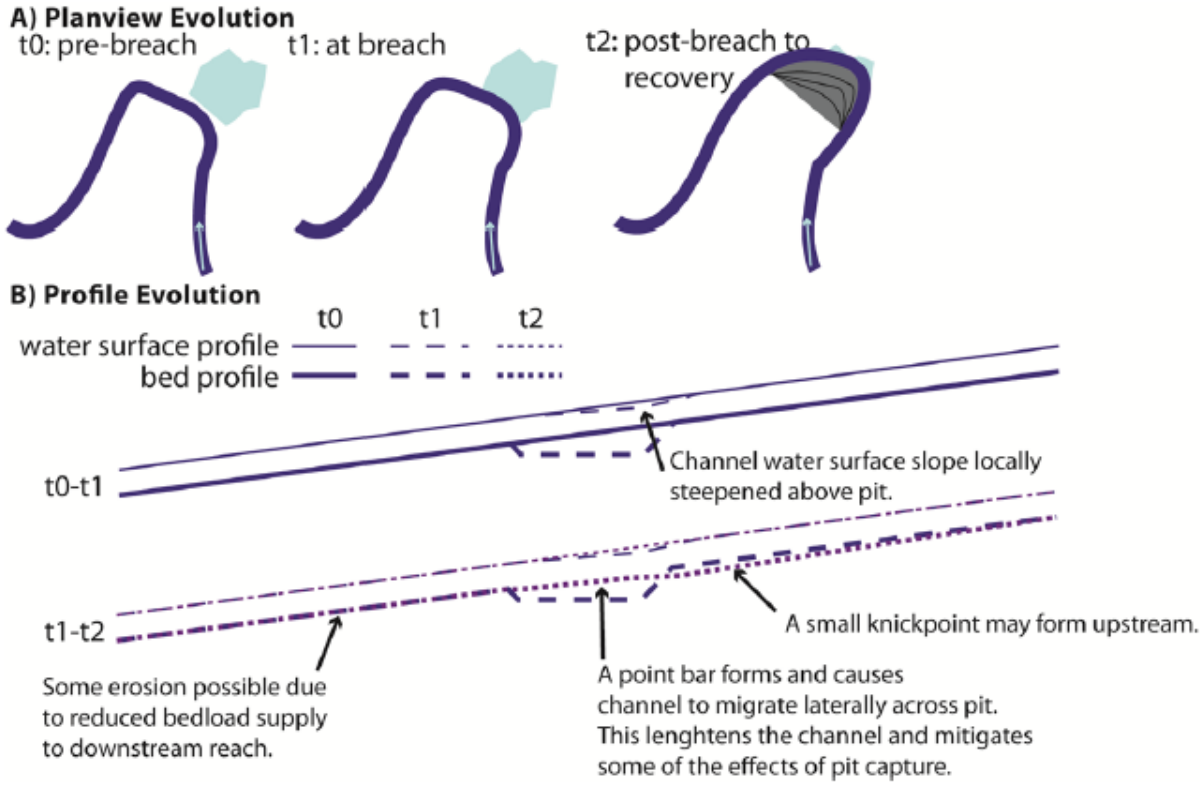

Figure 4.3: Schematic Illustration of plan view and profile response to a lateral connection between a river and a floodplain pit, from NHC (2014).

The different processes involved in gravel pit capture produce different principal hazards associated with avulsions and lateral connections. In an avulsion scenario, the channel is shortened, steepened, and expanded. All of which compound to drive steepening in the upstream reach, which results in a major potential for disturbance. In a lateral connection scenario, channel expansion is offset by channel lengthening, and there is usually less disturbance potential.

Because of the different potential responses to avulsion and lateral connection scenarios, it is useful to be able to predict which might be expected in a given location. NHC (2014) identified the slope ratio—calculated in a way to account for the shortening affect of the channel path through a pit— provided a useful parameter to predict the likelihood of avulsion. It is defined as the ratio of the slope of a possible avulsion path to the down channel slope. Slope ratios in the range from 3 to 5 —consistent with theoretical predictions of Slingerland and Smith (1998) are observed in naturally avulsing systems. Empirical evidence for the Yakima and other similar rivers in Washington and Oregon analyzed by NHC (2014) indicated that the average slope ratio of avulsions through floodplain pits was 3.2 (± 2.5 with a strongly positively skewed distribution). The average slope ratio for observed connections between a river and floodplain pit that did not result in avulsions was 1.5 (± 0.4), which was calculated to be significantly lower (t_{21}=-2.1, p=0.025) than the slope ratio associated with avulsions. The minimum slope ratio

where an avulsion occurred was 1.3. Results of a logistic regression (using the algorithm of Pezzullo 2014) also showed a strong relationship (X^2= 7.5; df=1; p= 0.0062) and indicated that an avulsion is possible at any slope ratio but that avulsion probability increases rapidly as the ratio increases from 1 to 2, as summarized in Table 4.2. Of course, engineering interventions can be designed to control energy dissipation and affect the expected outcome of a channel-to-pit connection scenario.

Table 4.2 Avulsion likelihood (following formal Intergovernmental Panel on Climate Change likelihood definitions) as a function of slope ratio, based on analysis of NHC (2014).

Slope Ratio Range	Avulsion through pit Likelihood
<1	Very Unlikely
1-1.4	Unlikely
1.4-2	About as likely as not
>2	Likely
3-4.5	Very Likely
>4	Extremely Likely

4.2 Evaluation of Reference Floodplain Pit Engagement Scenarios

Although many different scenarios for river-floodplain pit engagement are possible in the project area, a selection of eight possible scenarios were evaluated to understand the range of potential interactions between the river and the pits. These selected scenarios represent possible future developments of the river planform, possible design approaches, or combinations of these. This section analyzes the likely style and magnitude of channel response to each of these scenarios. The scenarios considered are illustrated in Figure 4.4 and key elements of their geometry are specified in Table 4.3. Each is also briefly described below.

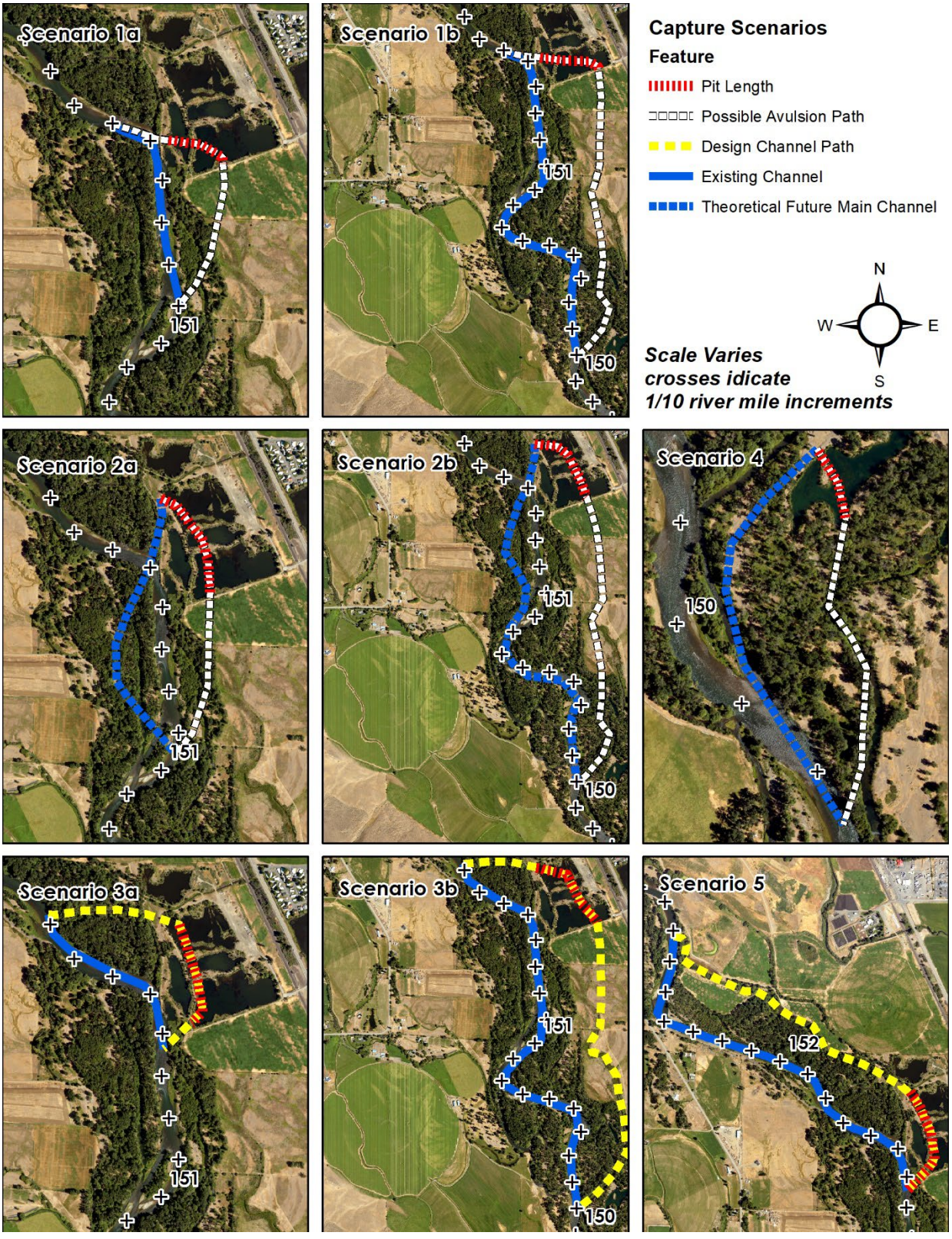

Figure 4.4: Geometry of Pit Capture Scenarios Described in the Text.

Table 4.3 Geometry of select potential floodplain pit engagement scenarios.

Scenario	Main Channel Length (X_{mc})	New channel length[1] (X_{nc})	Pit Length (X_{pit})	Connected Pit Volume (yd^3)	Slope Ratio[2]	Knickpoint Height (z, ft)[3]
1a	2574	3395	802	196,000	1.0	0
1b	7572	7882	1223	196,000	1.1	2
2a	3537	3515	1434	278,000	1.7	4
2b	7827	7594	1609	278,000	1.3	5
3a	2401	3447	1314	278,000	1.1	0.7
3b	8741	9483	1726	278,000	1.1	3
4	2218	2006	375	27,000	1.4	2
5	6989	7166	1978	278,000	1.3	5

Table Notes:

1)New channel length represents the possible length of the considered avulsion path or the length of a channel that may be intentionally constructed.

2) Slope ratio is calculated as the ratio between the effective avulsion path length and the main channel length, as follows: $\frac{X_{mc}}{X_{nc}-X_{pit}}$

3) Knickpoint height is calculated from the initial slope of the main channel (S_i) and difference between the current main channel length and effective avulsion path length, as follows: S_i (X_{mc} + X_{pit} – X_{nc})

Scenario1a: Downstream Pit Lateral Connection with Proximal Flow Return to Channel

This connection scenario plays out a very likely response to removal of the revetment berms between the Hansen Pits and the Channel where erosion breaches the berms between the river and the two most downstream (pits Center W and SE). Channel lengthening is proportional to the pit length engaged in this scenario, and so the slope ratio remains very close to 1, meaning avulsion development is very unlikely and minimal upstream knickpoint influence would be expected. The key geomorphic impacts of this scenario would be:

- A loss of bedload supply to the downstream channel equivalent to the connected pit volume, which may starve the downstream that channel of sediment supply for up to about 60 years.
- Create a high sinuosity meander that might aggressively migrate eastward towards the maintenance yards and road or into the intended future position of the spray field.

Scenario 1b: Downstream pit Lateral Connection with Breach on East Side

This connection scenario starts with the same engagement described in Scenario 1a but assumes a breach in the embankment of the downstream-most pit near the eastern margin, producing flow onto the floodplain that returns down valley across the existing spring-fed floodplain channel and fishhook side channel. Because this return flow path is lower sinuosity than the existing main channel, the slope ratio for this scenario is slightly higher than that in Scenario 1a. However at a value of 1.1, it is still considerably below the lowest slope ratio where a documented avulsion occurred in the review described by NHC (2014) (a slope ratio of 1.3). Based on the logistic regression, an avulsion remains possible at any slope ratio above 1. The low slope ratio and long flow path across the floodplain considered in the scenario, together, suggest that floodplain roughing measures (e.g. plantings, flood fencing, excavation of sinuous floodplain channels) or localized reinforcement of the berm below the pit to prevent failure during an overtopping event would likely effectively mitigate this hazard. Were this mitigated, the residual hazards would be the same as those specified for scenario 1a.

Scenario 2a: Future Meander Configuration Breaches Upstream Pit

Scenario 2a assumes a future meander configuration for the main channel where a meander apex breaches the upstream end of the upstream pit (pit N) and a relatively sinuous channel extends down valley, aligning the down valley channel-meander to the west and creating the opportunity for a higher cutoff ratio to form. This configuration is not especially likely given the current meander configuration and a normative tendency for down valley meander translation, but it provides a useful check on the range or expected response. The resulting slope ratio for these assumptions, 1.7, means that an avulsion through the pits would be about as likely as not, in this scenario. Assuming that avulsion develops, the relatively long length of the pit and main channel could result in the formation of a potentially consequential knickpoint (4 ft). Applying the framework on NHC (2014)[5] indicates this knickpoint would likely diffuse upstream over a distance of approximately 0.1 to 0.25 miles. The upstream migrating knickpoint would be expected to generate sediment for pit infilling

A variant on this scenario that was not evaluated could result from easterly channel migration of the main channel to the south of the pits, which could result in similar cutoff geometry to this scenario. That variant would be a likely outcome of the removal of the upstream right bank revetment (RM 151.8-152.4) and erosion of the berms along the left bank just downstream of the pits. In this case, however, the main channel would not be impinging against the pits on the upstream side, so it is also relatively unlikely. Given the connected pit volume and volume of

[5] Diffusion distance is estimated as follows $\frac{z}{t\,S_i}$, where t is a threshold slope difference between the knickpoint slope and the reach average slope where the knickpoint is no longer detectable. Ranges evaluated here use a value of t from 1.15 to 2. A value of t=2 is about as likely as not to be exceeded and a value of t=1.15 is very unlikely to be exceeded.

material that may be eroded from the upstream knickpoint, this scenario may affect bedload supply to the downstream channel for around 80 years.

Scenario 2b: Future Meander Configuration Breaches Upstream Pit and Downstream Pit Berm Breach forms on East Side

This connection scenario starts with the same engagement described in Scenario 2a, but a breach in the berm to the south of the downstream pit concentrates flow into the left bank floodplain and that flow returns to the main channel along a similar path to that described for Scenario 1b. This results in a slope ratio of 1.3, which suggests development of an avulsion would be unlikely. The long avulsion path adjacent to a relatively sinuous existing channel and long length of flow through the pits would form a relatively large knickpoint (~5 ft) which would be expected to diffuse over a distance of approximately 0.2 to 0.3 miles upstream. Given the connected pit volume and volume of material that may be eroded from the upstream knickpoint, this scenario may affect bedload supply to the downstream channel for around 70 years, although this would be substantially mitigated by supply of material from within the newly formed avulsion channel.

Scenario 3a and Scenario 3b: Designed Flow Through Channel

Scenario 3a assumes a small-to moderately sized side channel is intentionally routed through the pits, diverging from the existing channel about 0.4 miles upstream of the point where the channel currently impinges against the pits and returning to the mainstem channel at the downstream edge of the pits. Scenario 3b is similar but extends the constructed channel a long distance down the floodplain below the pits. This is a strategy that could result in fine sediment (sand and mud) settling into the pits to fill much of their volume through time, although it could also potentially create adverse ecological interactions between salmonids and warm water fish in the pits. Numerous positions of breaches between pits would be possible, but the pit length and new channel length would increase identically, so the single reference scenario encapsulates this range of potential options within the scenario. The low slope ratio for both of these scenarios (1.1) suggests that it would be unlikely to trigger an avulsion through the pits.

In this scenario, bed material transport into the pits would not be substantial, but the hydraulics within the pit would likely result in much of the suspended sediment transport of the flow through them settling out. Given the connected pit volume of 278,000 yd^3 and making the assumptions that:

- the designed channel would bring about 30% of the total suspended sediment yield (Table 3.2) into the pits,
- the trap efficiency for the pits for the sand fraction of that fine sediment is 90% and the silt and clay fraction of that fine sediment is 20%, and
- a bulk density of silty sand of 1.2 tons/yd^3

Then about 5,100 cubic yards of silty sand may accumulate in the pits annually which would allow them to naturally infill over a period of about 50 years.

Scenario 4: Future Channel Migration breaches "Camel Pit"

Scenario 4 assumes a future meander intersects "Camel Pit", the most riverward of the set of pits scattered across the floodplain at about PRM 150.1. This results in a high enough slope ratio that an avulsion through the pit would be about as likely as not. This avulsion would be expected to create an approximately 2-foot high knickpoint that would diffuse over a distance of approximately 300 to 500 feet upstream. Because of the relatively small volume of this pit, bed material transport would be expected to fill it within a decade.

Scenario 5: Schakke Side Channel routed through pits.

Scenario 5 assumes that the Schakke Side Channel 2 feature is extended and routed through Hansen Pits. Raw slope ratio (1.3) and knickpoint height estimates (5 ft) for this scenario likely overestimate the potential channel impacts because the pit connection would be at the downstream edge of a smaller side channel feature. Even so, the slope ratio suggests that it would be unlikely to result in an avulsion. Were an avulsion to occur, the "knickpoint" feature would be concentrated at the upstream edge of the pits, and likely diffuse before it propagated to the current channel location.

5 CONCLUSIONS AND DESIGN IMPLICATIONS

Overall, this analysis supports the design direction that NHC understands to be underway for the Lower Kittitas Reach Restoration Project. This analysis has found that relatively infrequent and large flows, which are reduced in the baseline condition compared to historic conditions, are important mechanisms for creating complex river and floodplain-channel morphology. In areas of high confinement, concentrated flow energy from these events tends to create a simple, narrow and deep channel, but in unconfined areas distributed flow on the floodplain during larger floods generates partial avulsions; this is the dominant side channel formation mechanism.

Floodplain sedimentation and side channel closure rates are slow, which means that complex morphology established during big flood events has a long-lasting legacy. Thus, floodplain channels excavated as a part of the proposed restoration project would be expected to persist for decades. Therefore, we expect substantial side and floodplain channel excavation to provide long-term habitat and river process benefits that help diffuse flood-flow energy. Diffused energy of future flood flows across the floodplain will help to maintain and enhance the system complexity-increasing dynamic that has been associated with those events in the past. That is because this will promote sediment retention in the main channel helping to drive lateral channel migration and maintenance relatively high-elevation hydraulic controls, promoting

continuing overbank flows with the potential to erode new floodplain and side channels (note that the importance of this process is illustrated by the contrast in geomorphic conditions between the PRM 153.8 to 152 sub-reach and PRM 150 to 152 sub-reach).

Most plausible pit connection scenarios would likely evolve as lateral connection scenarios rather than avulsions, with small to moderate local upstream effects on the channel profile. The combined volume of connected pits, however, is large compared to the bed material transport rate in the subject reach. This means that infilling of the pits, whether done by mechanical means or using natural sediment transport dynamics in the river, will be a large "sink" for the bed material sediment budget in the reach.

An additional scenario proposed by Inter-Fluve of partially filling the pits to mimic an abandoned oxbow with establishing connection to the mainstem channel at the downstream end and natural floodplain feature warrants continued design investigation. This scenario would function in a similar way to Scenario 3a, providing a hydraulic connection between the pits and the channel and high flow backwater inundation of Hansen Pits that would promote suspended load deposition for gradual pit infill, sustained off-channel habitat, and uplifted wetland conditions at the pit location. Preliminary analysis does not indicate that this creates an avulsion concern, and it may substantially reduce the amount of material needed for infilling the pits.

Report prepared by
Northwest Hydraulic Consultants Inc

Final to be signed by

Andrew Nelson, LG
Principal, Primary Author

Final to be signed by

Catherine Billor, PE
Staff Engineer, Field Observation Documentation

Report reviewed by

Final to be signed by

Peter Brooks, PE
Principal

NHC File Path: B:\2009321_Lower_Kittitas_Yakima_Restoration\80_Documentation

REFERENCES

Anderson, S., Sheibley, R., and Foreman, J. (2023). *Suspended-Sediment Data for the Yakima River at Kiona (USGS 12510500), Washington, June 2018 through September 2022 | U.S. Geological Survey*. [online] Available from: https://www.sciencebase.gov/catalog/item/64597b90d34ec179a836afd1 (Accessed 28 January 2025).

Church, M. (2006). Bed Material Transport and the Morphology of Alluvial River Channels. *Annual Review of Earth and Planetary Sciences*, 34(1), 325–354. doi:10.1146/annurev.earth.33.092203.122721.

Church, M., and Slaymaker, O. (1989). Disequilibrium of Holocene sediment yield in glaciated British Columbia. *Nature*, 337(6206), 452–454. doi:10.1038/337452a0.

Davidson, S. L., and Eaton, B. C. (2018). Beyond Regime: A Stochastic Model of Floods, Bank Erosion, and Channel Migration. *Water Resources Research*. doi:10.1029/2017WR022059. [online] Available from: http://doi.wiley.com/10.1029/2017WR022059 (Accessed 13 September 2018).

Eaton, B. C. (2006). Bank stability analysis for regime models of vegetated gravel bed rivers. *Earth Surface Processes and Landforms*, 31(11), 1438–1444.

Eaton, B. C. (2007a). *The University of British Columbia Regime Model (UBCRM)- User's manual: Draft*. University of British Columbia. Vancouver, BC pp.

Eaton, B. C. (2007b). *The University of British Columbia Regive Model (UBCRM) User's Manual*.

Eaton, B. C., Church, M., and Millar, R. G. (2004). Rational regime model of alluvial channel morphology and response. *Earth Surface Processes and Landforms*, 29(4), 511–529.

Eaton, B. C., Millar, R. G., and Davidson, S. (2010). Channel patterns: Braided, anabranching, and single-thread. *Geomorphology*, 120(3–4), 353–364. doi:10.1016/j.geomorph.2010.04.010.

Eaton, B., and Millar, R. (2017). Predicting gravel bed river response to environmental change: the strengths and limitations of a regime-based approach. *Earth Surface Processes and Landforms*, 42(6), 994–1008. doi:10.1002/esp.4058.

Fryirs, K. A., Wheaton, J. M., and Brierley, G. J. (2016). An approach for measuring confinement and assessing the influence of valley setting on river forms and processes: Measuring Confinement along Fluvial Corridors. *Earth Surface Processes and Landforms*, 41(5), 701–710. doi:10.1002/esp.3893.

GeoEngineers (2025). *Preliminary Geotechnical and Geological Engineering Services: Hansen Floodplain Restoration Project Kittitas County, Washington*. Report Prepared by GeoEngineers for Kittitas County.

Hilldale, R. C., and Godaire, J. E. (2010). *Yakima River Geomorphology and Sediment Transport Study: Gap to Gap Reach, Yakima, WA* (SRH-2010-08). Report prepared by Bureau of Reclamation Technical Service Center for the County of Yakima, WA. Bureau of Reclamation, Denver, CO. [online] Available from: http://www.usbr.gov/pmts/sediment/projects/Yakima/download/Gap2Gap_Study_Final_02142011.pdf (Accessed 21 July 2014).

Millar, R., Eaton, B., and Church, M. (2014). *UBC Regime Model*. [online] Available from: http://ibis.geog.ubc.ca/~beaton/UBC%20Regime%20Model.html (Accessed 19 March 2015).

Nelson, A., McLean, D., Brooks, P., and Hodges, K. (2015). Quantifying the Risk of Floodplain Mine Pit Capture Along Gravel Bedded Streams of the PNW. Stevenson, WA. [online]

Available from: http://www.rrnw.org/wp-content/uploads/2015Nelson_Andrew_Session3.pdf.

Nelson, L. M. (1973). *Sediment transport by streams in the Upper Columbia River Basin, Washington, May 1969-June 1971* (73–39). USGS Numbered Series. U.S. Geological Survey. [online] Available from: http://pubs.er.usgs.gov/publication/wri7339 (Accessed 18 November 2021).

NHC (2014). *Uncontrolled Pit Capture Likelihood and Risk- DRAFT* (21792). Memorandum prepared by Northwest Hydraulic Consultants for Yakima County Water Rescources Division.

Pitlick, J., Wilcock, P., and Cui, Y. (2009). *BAGS: Bedload Assessment in Gravel-bedded Streams*. [online] Available from: http://www.stream.fs.fed.us/publications/bags.html.

Stevens, M. A., and Nordin, C. F. (1990). First Step Away from Laceye's Regime Equations. *Journal of Hydraulic Engineering*, 116(11), 1422–1425. doi:10.1061/(ASCE)0733-9429(1990)116:11(1422).

Sumioka, S. S., Kresch, D. L., and Kasnick, K. D. (1998). *Magnitude and frequency of floods in Washington* (97–4277). Water-Resources Investigations Report. US Department of the Interior, US Geological Survey, prepared in cooperation with Washington State Department of Transportation and Washington State Department of Ecology, Tacoma, WA. 91 pp. [online] Available from: http://pubs.usgs.gov/wri/1997/4277/report.pdf (Accessed 11 December 2014).

USBR (2024). *Lower Kittitas Reach Floodplain Reconnection Project Concept Basis Of Design Report*.

WSE (2021). *Hansen Pits Channel Migration and Avulsion Risk Assessment*. Report prepared by Watershed Science and Engineering for Kittitas County Public Works.

DISCLAIMER

This document has been prepared by **Northwest Hydraulic Consultants Inc.** in accordance with generally accepted engineering practices and is intended for the exclusive use and benefit of Kittitas County and Inter-Fluve, Inc. and their authorized representatives for specific application to the Lower Kittitas Reach Floodplain Reconnection Project along the Yakima River near Ellensburg, WA. The contents of this document are not to be relied upon or used, in whole or in part, by or for the benefit of others without specific written authorization from **Northwest Hydraulic Consultants Inc**.. No other warranty, expressed or implied, is made.

Northwest Hydraulic Consultants Inc. and its officers, directors, employees, and agents assume no responsibility for the reliance upon this document or any of its contents by any parties other than Kittitas County and Inter-Fluve, Inc.

APPENDIX A

FIELD OBSERVATIONS MAP SET